Supplemental Figures

Supplemental Figure 1. Th22 cells accumulated in gastric mucosa of *H. pylori*-infected patients and mice. (A and B) Dynamic change of Th22 cell response (A) and IL-22 mRNA expression (B) in WT *H. pylori*- infected, *ΔcagA*-infected, and uninfected C57BL/6 mice. (C and D) Concentrations of IL-22 protein in gastric mucosa of WT *H. pylori*-infected, *ΔcagA*-infected, and uninfected BALB/c mice (C) and C57BL/6 mice (D) on day 35 p.i. were compared. (E) Representative dot plots of intracellular cytokine staining for IL- 22 expression on immune cell types (including NK cells, lymphoid tissue inducer-like cells (LTi-like cells), innate lymphoid cells, and Th cells) among total $CD45^+$ haematopoietic cells in gastric mucosa of WT *H. pylori*-infected BALB/c mice on day 35 p.i.. Red histograms represent cells stained for specific markers; blue histograms represent cells stained with isotype control Ab. n=5 per group per time point in *A* and *B*. *p<0.05, **p<0.01 for groups connected by horizontal lines compared, or compared with uninfected mice.

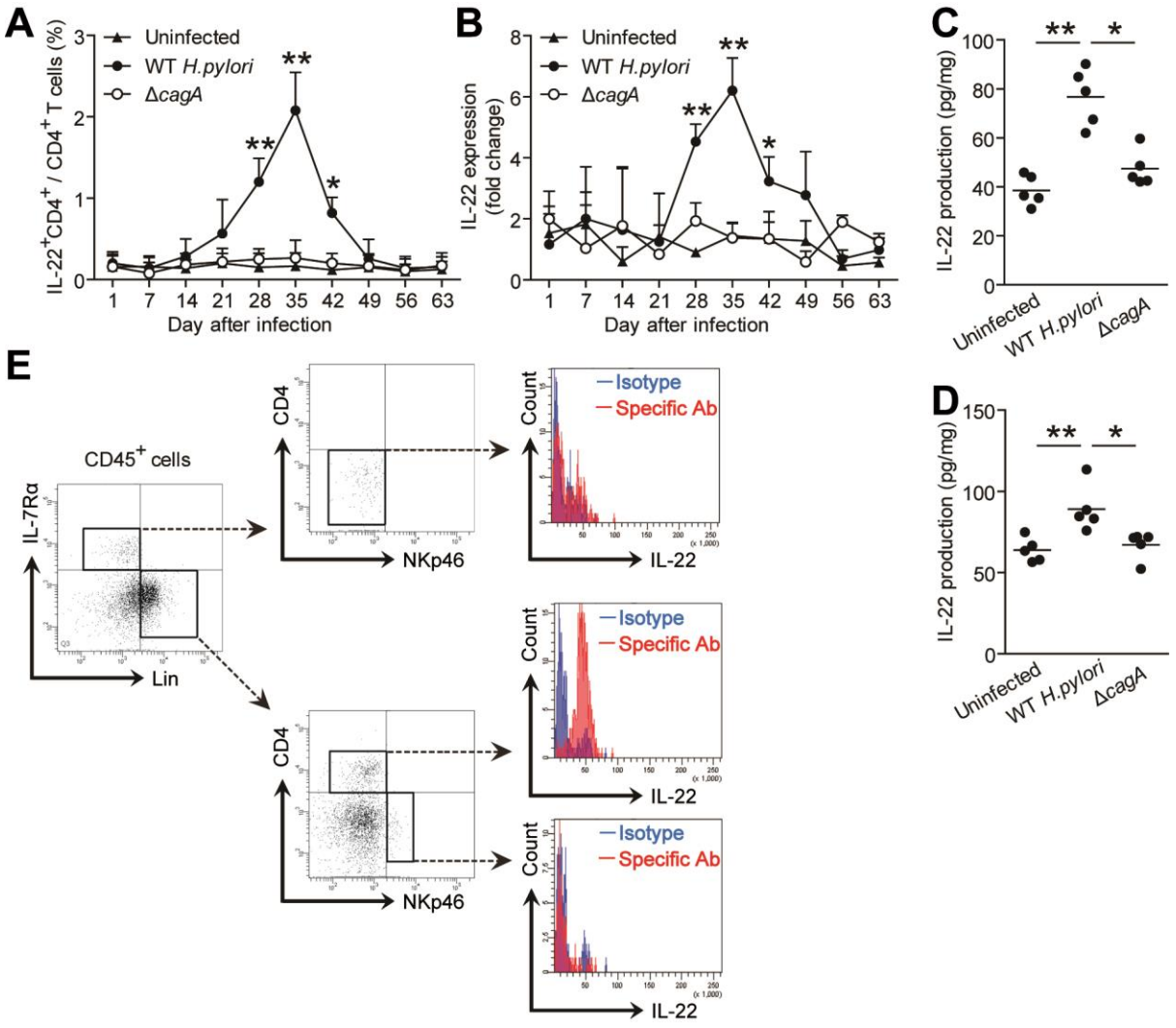

Supplemental Figure 2. Dynamic change of Th22 cell response in BM, blood, spleen mesenteric lymph node, and Peyer's pathes of WT *H. pylori*-infected, *ΔcagA*-infected, and uninfected BALB/c (A) and C57BL/6 (B) mice. Results are expressed as mean ± SEM. n=5 per group per time point.

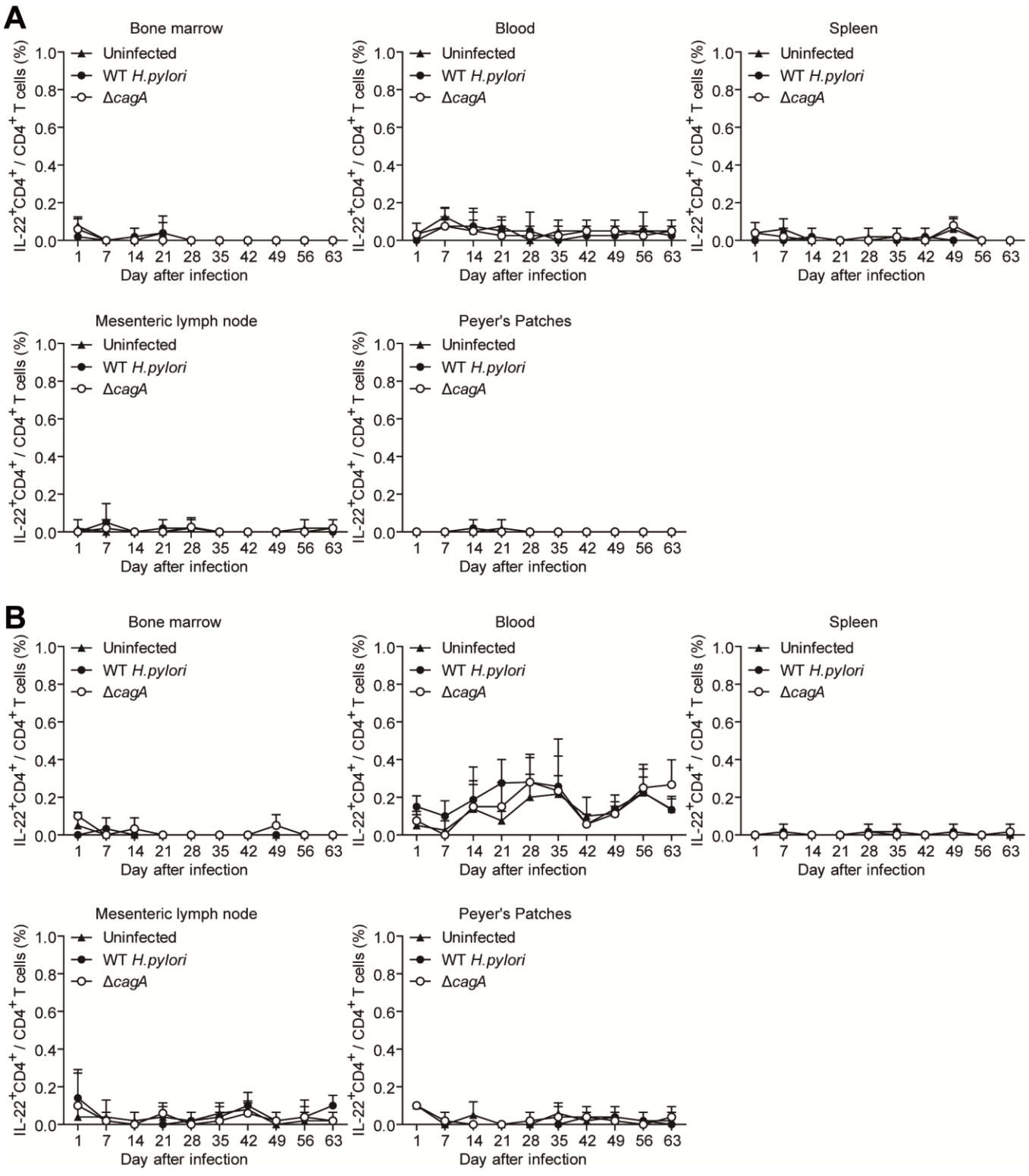

Supplemental Figure 3. IL-22 has pro-inflammatory effects during *H. pylori* infection, and *H. pylori* induces gastric epithelial cells to up-regulate IL-22R1. (A) Histological scores of inflammation in gastric antra of WT *H. pylori*-infected BM chimera mice on day 49 p.i. were compared. (B) Dynamic change of IL-22R1 mRNA expression in WT *H. pylori*-infected, *ΔcagA*-infected, and uninfected C57BL/6 mice. n=5 per group per time point. (C) IL-22R1 protein in gastric mucosa of

cagA^{+} *H. pylori*-infected and *cagA*$^{-}$ *H. pylori*-infected patients was analyzed by Western blot. (D) IL-22R1 protein in WT *H. pylori*-infected, *ΔcagA*-infected, and uninfected AGS cells was analyzed by Western blot. n=5 per group per time point in *B*. *p<0.05, **p<0.01 for groups compared with uninfected mice.

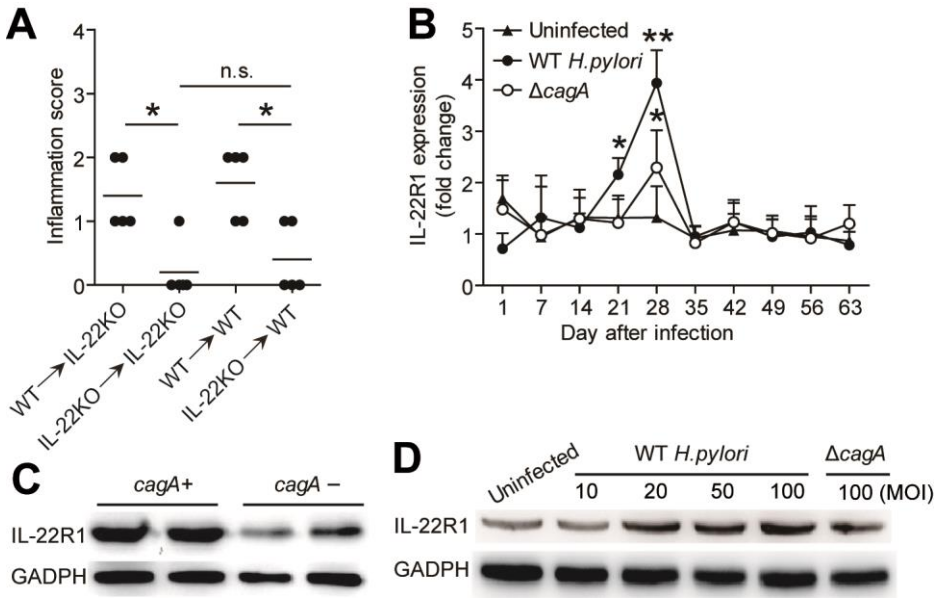

Supplemental Figure 4. IL-22 promotes CXCL2 production, and CXCR2-expressing MDSCs accumulated in gastric mucosa during *H. pylori* infection. (A) Expression of CXCL2 mRNA in unstimulated or IL-22-stimulated AGS cells was compared (n=3). (B) CXCL2 mRNA expression in unstimulated, or IL-22- stimulated primary gastric epithelial cells from uninfected donors were compared (n=3). (C) Dynamic change of MDSCs in WT *H. pylori*-infected, *ΔcagA*-infected, and uninfected C57BL/6 mice. n=5 per group per time point. (D) Representative immunofluorescence staining images showed M-MDSCs infiltration in gastric mucosa of WT *H. pylori*-infected mice on day 49 p.i.. Scale bars: 20 microns. *p<0.05, **p<0.01, n.s p>0.05 for groups connected by horizontal lines compared, or compared with uninfected mice.

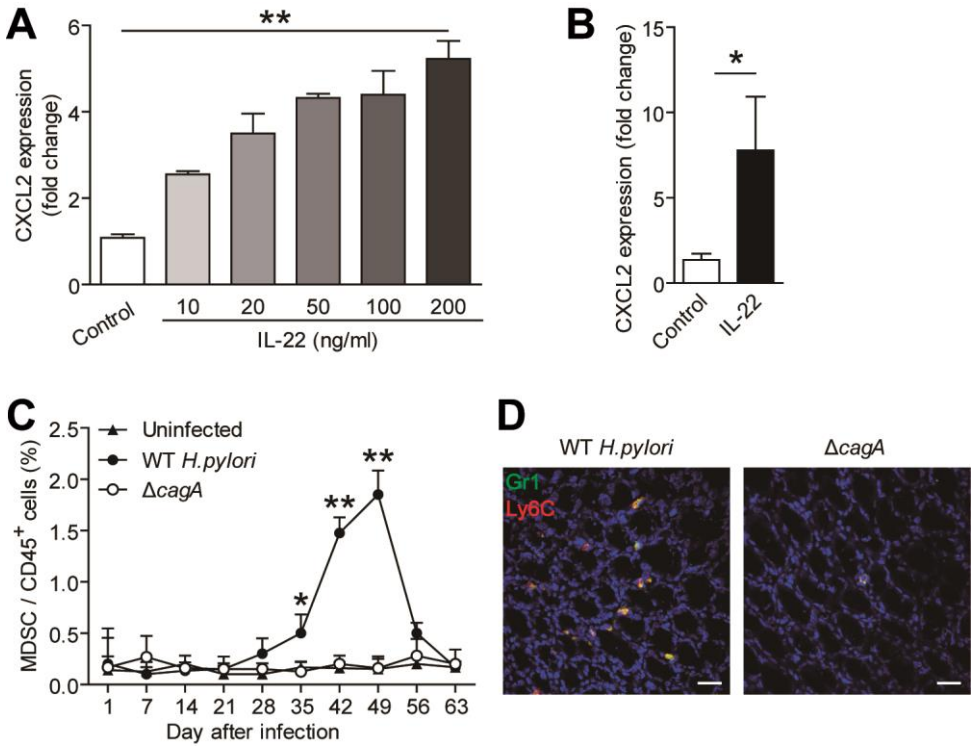

Supplemental Figure 5. IL-22 promotes MDSC accumulation in *H. pylori*-infected gastric mucosa by CXCL2-CXCR2 axis *in vivo*. (A) MDSC responses in gastric mucosa of WT *H. pylori*-infected WT BALB/c (left) and WT C57BL/6 (right) mice injected with Abs against IL-22, IL-17A, IL-17F, or IFN-γ or isotype control Abs on day 49 p.i. were compared. (B) MDSC responses in gastric mucosa of in WT *H. pylori*- infected WT C57BL/6 mice injected with IL-22 or PBS control, Abs against IL-22 (IgG2a), CXCR2 (IgG2a), and/or CXCL2 (IgG2b) or corresponding isotype control Abs, or SB225002 or DMSO control on day 49 p.i. were compared. (C) MDSC responses in gastric mucosa of WT *H. pylori*-infected BM chimera mice on day 49 p.i. were compared. *p<0.05, **p<0.01, n.s p>0.05 for groups connected by horizontal lines compared.

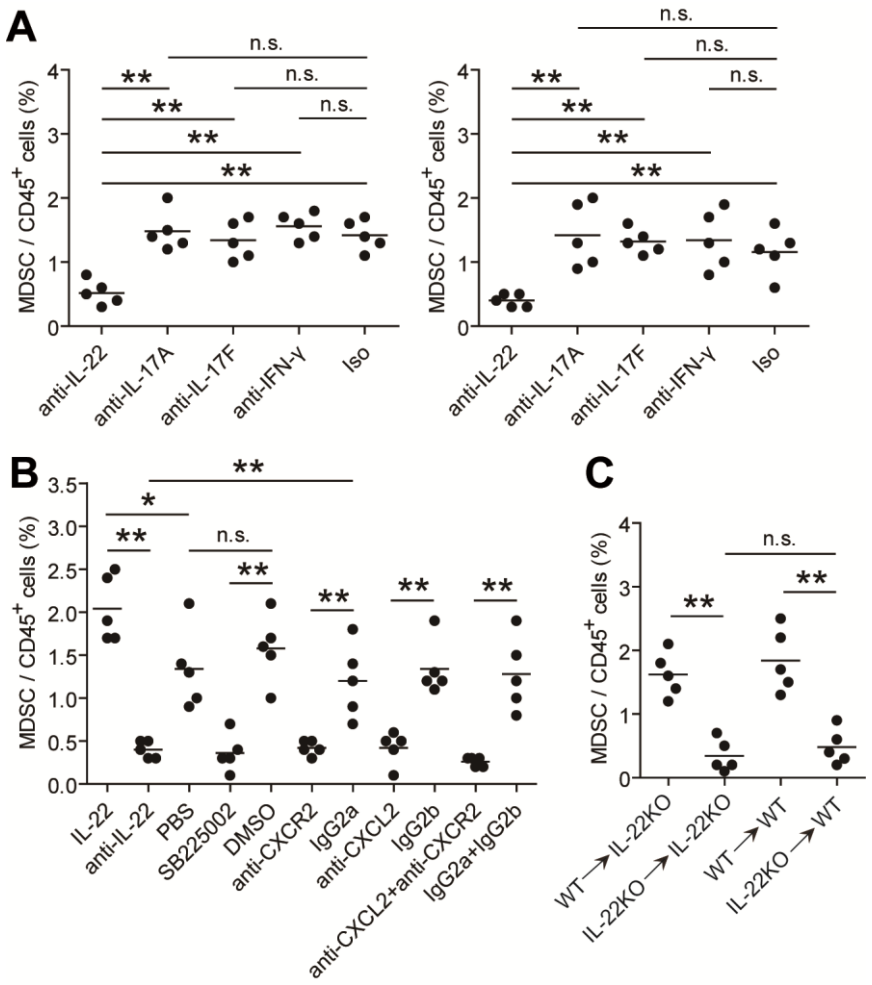

Supplemental Figure 6. IL-22 regulates pro-inflammatory proteins S100A8 and S100A9 expression. (A) Correlations between IL-22 and S100A8 or S100A9 in gastric mucosa of *H. pylori*-infected patients were analyzed. (B) Clustering of microarray data for the genes in human $CD45^{+}CD14^{+}HLA\text{-}DR^{low/-}$ MDSCs. (C and D) Dynamic change of S100A8 and S100A mRNA expression in WT *H. pylori*-infected, *ΔcagA*-infected, and uninfected BALB/c (C) and C57BL/6 (D) mice. (E) S100A8 and S100A9 proteins in gastric mucosa of WT *H. pylori*-infected, *ΔcagA*-infected, and uninfected BALB/c mice on day 49 p.i. were analyzed. (F) S100A8 and S100A9 protein concentrations in gastric mucosa of WT *H. pylori*-infected BM chimera mice on day 49 p.i. were compared. (G) Representative dot plots of MDSCs and expression of IL-22R1 on MDSCs by gating on $CD45^{+}$ cells in peripheral blood of *H. pylori*-infected patients. n=5 per group per time point in *C* and *D*. *p<0.05, **p<0.01, n.s p>0.05 for groups connected by horizontal lines compared, or compared with uninfected mice.

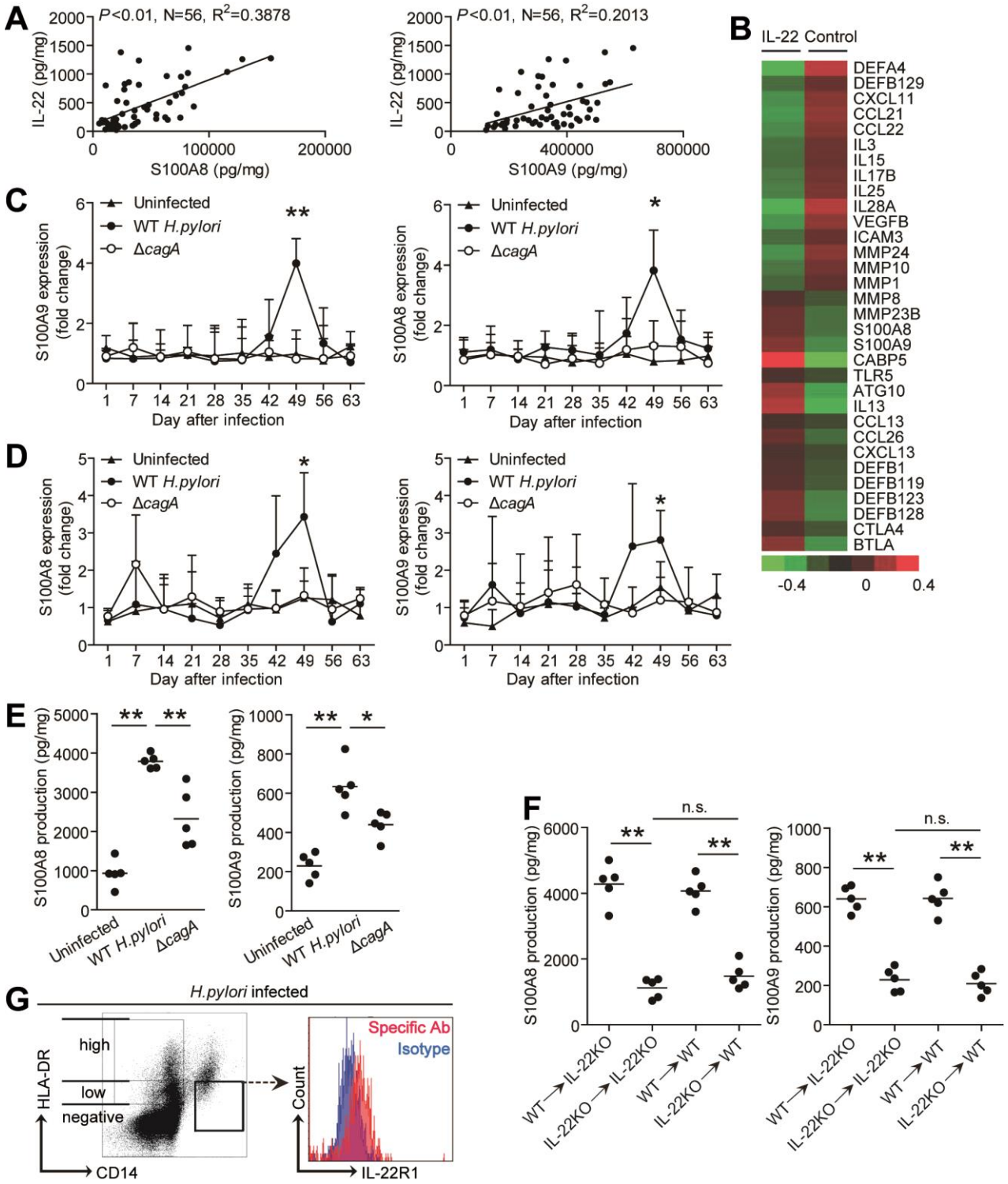

Supplemental Figure 7. IL-22-induced MDSCs suppress Th1 cell response in H. pylori infection. (A and B) Th1 cell responses in gastric mucosa of in H. pylori-infected WT C57BL/6 mice injected with IL-22 or PBS control, Abs against IL-22 (IgG2a), CXCR2 (IgG2a), and/or CXCL2 (IgG2b) or corresponding isotype control Abs, or SB225002 (the potent and selective nonpeptide CXCR2 antagonist) or DMSO control (A), or H. pylori-infected BM chimera mice (B) on day 49 p.i. were compared. (C) CFSE-labelled peripheral CD4+ T cells of uninfected donors were co-cultured for 5 days with human peripheral CD45+CD14+HLA-DRlow/- MDSCs from H. pylori-infected patients at different ratios. Production of IFN-? was detected by ELISA in the co-culture supernatants (n=3). *p<0.05, **p<0.01, n.s p>0.05 for groups connected by horizontal

lines compared.